npj | biofilms and microbiomes

Article

Published in partnership with Nanyang Technological University

https://doi.org/10.1038/s41522-025-00835-2

Engineered *Mycoplasma pneumoniae* targeting dual-species bacterial biofilms: a novel strategy against infections

Rocco Mazzolini[1,2] ✉, Victoria Garrido[3,7], Andromeda-Celeste Gomez[2,4,7], Maria Collantes[5,6], Maria Jesús Grilló[3], Carlos Piñero-Lambea[1,2], Isidre Gibert[2,4], Daniel Yero[2,4] & Maria Lluch-Senar[1,2] ✉

Antimicrobial resistance is a major global health threat, potentially causing 8.22 million deaths annually by 2050. Polymicrobial biofilms significantly contribute to this crisis, leading to treatment failure, especially in chronic airway infections caused by *Staphylococcus aureus* and *Pseudomonas aeruginosa*, common in ventilator-associated pneumonia and cystic fibrosis. To address this, we engineered an attenuated *Mycoplasma pneumoniae* strain, CV8_HAD, to secrete biofilm-disrupting enzymes (PelAh, PslGh, A1-II' and Dispersin B). CV8_HAD showed strong in vitro activity against single and mixed-species biofilms of *S. aureus* and *P. aeruginosa*, and demonstrated in vivo efficacy against *S. aureus* biofilms in mice and mixed infections in *Galleria mellonella* larvae. This study establishes engineered *M. pneumoniae* as a promising therapeutic strategy for tackling microbial biofilms and highlights the potential of G. *mellonella* larvae models as an alternative to mouse models in advancing research on biofilm-targeting interventions.

Antimicrobial resistance (AMR) represents a critical global challenge to public health and development. Recent studies reported a concerning rise in AMR-related deaths in 2021 (i.e. 4.71 million deaths associated with AMR), foreseeing up to 8.22 million deaths globally by 2050[1]. The six primary bacterial pathogens associated with resistance-related mortality are *Escherichia coli*, *Staphylococcus aureus*, *Klebsiella pneumoniae*, *Streptococcus pneumoniae*, *Acinetobacter baumannii*, and *Pseudomonas aeruginosa*. These six species are on the WHO bacterial priority pathogens list[2]. The pathogenicity of these bacteria is closely linked to their ability to form biofilms, i.e. structured microbial communities encased in a self-produced polymeric matrix that can colonize both biotic and abiotic surfaces. The extracellular matrix of biofilms comprises diverse exopolymeric substances, including polysaccharides, proteins, DNA, and lipids, predominantly synthesized by the microorganisms[3]. Once established, bacterial biofilms can evade host immune responses and exhibit heightened antibiotic resistance, posing a more significant threat to human health than planktonic bacteria. Biofilm formation is strongly associated with persistent and chronic infections, and it is estimated that 65–80% of hospital-acquired infections are biofilm-related[4,5].

In respiratory diseases, *S. aureus* and *P. aeruginosa* stand out as the most frequent dual-species biofilms, linked to ventilator-associated pneumonia (VAP)[6–8], cystic fibrosis (CF)[9,10], chronic obstructive pulmonary disease (COPD)[11], bronchiectasis[12], and tracheobronchitis[13]. Since *S. aureus* and *P. aeruginosa* frequently coexist in multi-species biofilms, their interaction has been extensively studied in vitro and in vivo. When grown together in vitro under nutrient-limited conditions, *P. aeruginosa* typically outcompetes *S. aureus* by producing anti-staphylococcal factors controlled by the quorum sensing[14–16]. However, in vivo, these two species cooperate by enhancing colonization and decreasing susceptibility to a range of clinically relevant antibiotics[13,17–22], ultimately leading to worse clinical outcomes compared to those observed in single species infections[13,21,23–26].

Given the complexity of multi-species biofilms in respiratory diseases, a better outcome relies on therapies capable of degrading the extracellular matrix produced by multiple bacteria. While many approaches for targeting *S. aureus*[27–32] or *P. aeruginosa*[33,34] in individual biofilms were reported with promising results against monocultures, their efficiency against polymicrobial biofilms remains questionable[35]. Furthermore, the need to combine various compounds, such as antiseptics, antibiotics, EDTA, and proteases to achieve a synergistic antibiofilm effect[28,35–38] presents logistical and cost limitations, emphasizing the value of a single treatment capable of delivering multiple agents simultaneously and in situ. In this context, engineered bacteria are promising tools due to their capacity to colonize

[1]Pulmobiotics Ltd, Barcelona, Spain. [2]Institute of Biotechnology and Biomedicine (IBB), UAB, Barcelona, Spain. [3]Institute of Agrobiotechnology, CSIC-Navarra Government, Mutilva, Spain. [4]Department of Genetics and Microbiology. Universitat Autònoma de Barcelona (UAB), Barcelona, Spain. [5]Translational Molecular Imaging Unit (UNIMTRA), Nuclear Medicine-Department, Clínica Universidad de Navarra, Pamplona, Spain. [6]IdiSNA, Navarra Institute for Health Research, Pamplona, Spain. [7]These authors contributed equally: Victoria Garrido, Andromeda-Celeste Gomez. ✉e-mail: rocco.mazzolini@uab.cat; maria.lluch@uab.cat

specific tissues and to deliver multiple biologically active molecules in situ[39]. Recently, we described an innovative strategy able to destroy monoculture biofilms in vivo in a preclinical mouse model, by using an engineered non-virulent minimal bacterium derived from *Mycoplasma pneumoniae*[32,33]. Importantly, the absence of a cell wall in *M. pneumoniae* allows the use of engineered therapeutical *M. pneumoniae* strains degrading the biofilms together with antibiotics that target the cell wall components of pathogenic bacteria.

Despite promising in vivo results of engineered *M. pneumoniae* strains against biofilms formed by *S. aureus* or *P. aeruginosa*[32,33], the potential of this novel approach against multispecies biofilms has not been explored. Here, we report the engineering of a new therapeutic *M. pneumoniae* attenuated strain, namely CV8_HAD. In contrast to previously described therapeutic strains[32,33], CV8_HAD is designed to simultaneously secrete a set of enzymes (PelAh, PslGh, AI-II' and Dispersin B) that disrupt *S. aureus* and *P. aeruginosa* dual-species biofilms, thereby broadening its potential clinical applications. First, we assessed the antibiofilm activity of CV8_HAD against single and dual-species biofilms in vitro. Then, we characterized its activity in vivo using *Galleria mellonella* larvae: in this versatile, cost-effective, and ethically advantageous model we found an increase in the survival rate of larvae infected with *P. aeruginosa* alone or in combination with *S. aureus*.

In conclusion, we present an engineered lung bacterium that dissolves complex biofilms as a solution to treat resistance to antibiotics in respiratory infectious diseases.

Results

Rational engineering of *Mycoplasma pneumoniae* strain CV8_HAD

To generate the CV8_HAD strain, we introduced four genes encoding biofilm-degrading enzymes into the genome of the attenuated *M. pneumoniae* strain CV8[40] via transposon mutagenesis. Specifically, as schematized in Fig. 1a, we incorporated: the hydrolytic PelAh and PslGh domains of the glycoside hydrolases from *P. aeruginosa*, that target the Pel and Psl exopolysaccharides (payload H); the alginate lyase A1-II′ from *Sphingomonas* sp., targeting alginate homo- and heteropolymers[41] (payload A); and the glycoside hydrolase Dispersin B from *Aggregatibacter actinomycetemcomitans*, targeting the exopolysaccharide PNAG (payload D). Also, the CV8_HA and CV8_D single mutants were built and used as controls. To enable release into the supernatant (SN), the proteins were fused to the optimized secretion signal MPN142_OPT[32]. Western blot analysis confirmed their presence in both cell lysates and the SN (Fig. 1b). The payloads expression and secretion did not affect the in vitro growth rate (as determined by growth curves, Supplementary Fig. 1a) or the in vivo persistence of the strains in murine lungs (Supplementary Fig. 1b).

CV8_HAD degrades multispecies biofilms in vitro

To validate the antibiofilm efficacy of the payloads carried by CV8_HAD, we incubated SN samples from CV8 strains to 24h-mature biofilms preformed in vitro by *S. aureus* strain Sa15981[42,43], a strong biofilm producer, or *P. aeruginosa* lab-standard strain PAO1. Quantification of biofilm degradation using the crystal violet method showed that the CV8_D carrying only payload D specifically degraded *S. aureus* biofilm (90% degradation compared to the control strain CV8), CV8_HA carrying payloads H and A specifically degraded *P. aeruginosa* (57% degradation), while CV8_HAD degraded both *S. aureus* and *P. aeruginosa* (90% and 63% degradation, respectively) (Fig. 1c, 1d).

To broaden the potential clinical applications of CV8_HAD, we further validated its antibiofilm efficacy against a panel of five additional *P. aeruginosa* and *S. aureus* strains isolated from patients with tracheobronchitis or bronchial colonization (Table 1) and one *S. aureus* (SAR10471) isolated from a patient co-infected with *P. aeruginosa* (PAR10471). This experiment confirmed the antibiofilm activity of CV8_HAD in a variety of *P. aeruginosa* clinical isolates; however, it could not be evaluated in SAR10471, as this strain did not exhibit detectable biofilm formation (Supplementary Fig. 2).

After confirming the antibiofilm activity of CV8_HAD, we next tested its antimicrobial effects. Growth of *P. aeruginosa* and *S. aureus* in the presence of CV8_HAD SN did not show a significant delay compared to CV8 SN, demonstrating that CV8_HAD payloads do not directly inhibit bacterial proliferation (Supplementary Fig. 3).

Since *P. aeruginosa* and *S. aureus* are frequently co-isolated from biofilm-associated respiratory diseases[13,21], we next investigated the potential of CV8_HAD SN to dissolve mixed biofilms. First, we produced dual-species biofilms using two different strain combinations: (1) a mixture of the

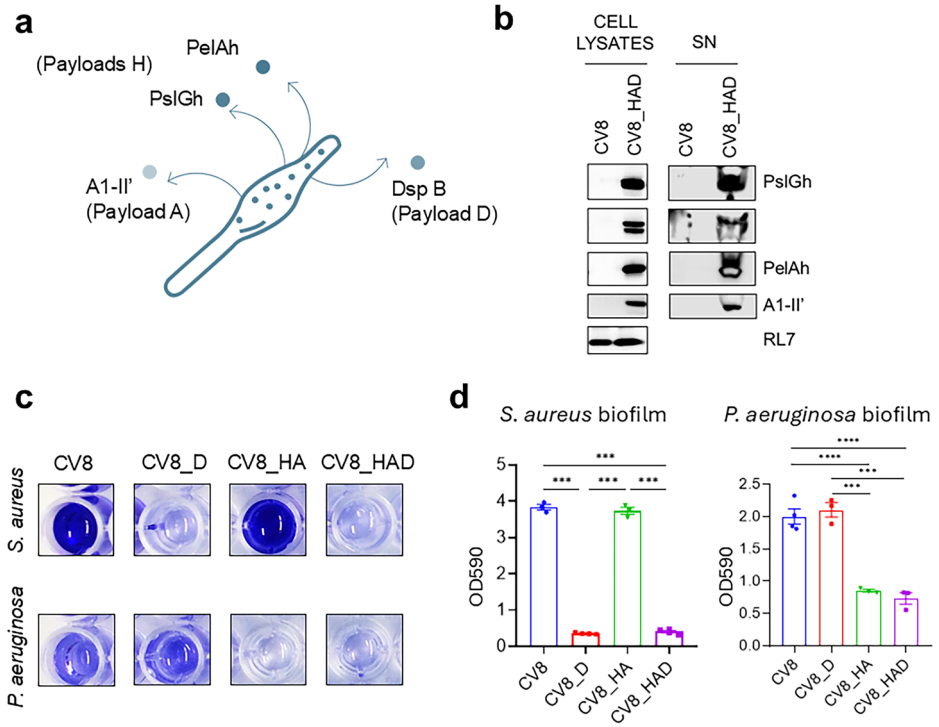

Fig. 1 | CV8_HAD strain dissolves *S. aureus* and *P. aeruginosa* biofilms in vitro. a Graphical representation of the antibiofilm payloads secreted by *M. pneumoniae* strain CV8_HAD. **b** Western blot analysis of CV8_HAD lysate and supernatant (SN) showing expression of the payloads; the CV8 chassis and the loaded ribosomal protein RL7 were used as controls. **c** Representative images of crystal violet assays used to quantify *S. aureus* (strain Sa15981) or *P. aeruginosa* (strain PAO1) biofilms after treating with SN from CV8 strains. CV8_D expresses payload D only; CV8_HA expresses payloads H and A. **d** Plot showing the quantification of biofilm dissolution by CV8 strains SN treatments in vitro, using the crystal violet assay. Data are shown as the mean of three independent experiments ± SEM. ***$p < 0.001$, ****$p < 0.0001$ by one-way Anova followed by the post-hoc Tukey's multiple comparison tests.

lab-standard strain PAO1 and the clinical isolate Sa15981, and (2) a mixture of the clinical co-isolated strains PAR10471 and SAR10471[13]. For each combination, we inoculated *S. aureus* and *P. aeruginosa* at a CFU ratio of 4:1, to prevent *P. aeruginosa* from totally outcompeting *S. aureus* as previously observed[13]. This approach resulted in a robust multispecies biofilm formation after 24 h. These biofilms were then incubated for six additional hours with either CV8_HAD or CV8 supernatants. Crystal violet staining revealed that CV8_HAD SN significantly degraded both dual-species biofilms compared to the CV8 control SN, with 93% degradation of mixture 1 (Fig. 2a) and 68% degradation of mixture 2 (Fig. 2c). This bacterial biomass reduction was accompanied by more than 2 logs reduction in *S. aureus* CFU, with no statistical impact on *P. aeruginosa* CFU reduction under these experimental conditions (Figs. 2b and 2d).

These data demonstrate that CV8_HAD dissolves mixed biofilms of *P. aeruginosa* and *S. aureus* in vitro.

Table 1 | Bacterial strains

Bacteria	Strain	Reference
Mycoplasma pneumoniae strain M129	CV8	40
	CV8_HAD	This work
	CV8_HA	
	CV8_D	
Pseudomonas aeruginosa	PAO1	ATCC #47085*
	PAR10471	13
	PAR7244	
	PAR2746	
	PAR7115	
	PAR5091	
Staphylococcus aureus	Sa15981	43
	SAR10471	13

*ATCC American Type Culture Collection.

CV8_HAD suppresses infections in *Galleria mellonella* larvae

After demonstrating that CV8_HAD dissolved dual-species biofilms in vitro, we sought to test its anti-biofilm activity in vivo. Although we succeeded to validate CV8_HAD anti-biofilm activity in a well-characterized murine model of subcutaneous *S. aureus* biofilm (Supplementary Fig. 4), we were unable to identify a reliable murine model of dual-species biofilm. Therefore, we set out to establish an alternative in vivo infection model using *G. mellonella* (greater wax moth) larvae to add data on the potential applications of our engineered strain. This extensively characterized invertebrate organism has been demonstrated as a suitable model for studying microbial infections and antimicrobial agents efficacy, allowing for faster and more versatile screening while requiring simpler infrastructure and no animal welfare or ethical approvals[44].

First, the toxicity of CV8_HAD was evaluated by inoculating larvae ($n = 15$) with increasing doses of CV8_HAD ranking from 10^6 to 10^8 CFU/larva, and monitoring larval survival over eight days. A group of larvae ($n = 15$) inoculated with 3×10^2 CFU/larva of *P. aeruginosa* strain PAR7244, was used as a virulence control, since it provides 100% lethality in 4 days. The results showed that all larvae inoculated with CV8_HAD survived in healthy condition until the end of the experiment (8 days post inoculation, dpi, Supplementary Fig. 5a), exhibiting no clinical symptoms such as reduced movement, failure to form a cocoon, or melanization, therefore demonstrating that CV8_HAD is non-virulent in this model even at the higher dose administered. Interestingly, although CV8_HAD persistence decreases by three orders of magnitude beyond 24 h (Supplementary Fig. 5b), viable cells were still detectable in larvae up to three dpi.

Second, the therapeutic efficacy of CV8_HAD was evaluated in larvae infected with *P. aeruginosa* and/or *S. aureus*. Treatments were administered either 1 or 24 h post-infection (hpi) (Fig. 3a), and larval survival was monitored for eight days. In PAR10471-infected larvae, CV8_HAD increased the median survival compared to the control when administered at both 1 hpi (seven days in CV8_HAD group vs. three days in CV8 controls) and 24 hpi (more than 50% of the larvae were still alive at the end of the study, vs. three days; Fig. 3b). In SAR10471-infected larvae, treatment with CV8_HAD had no significant effect on survival when administered at 1 hpi,

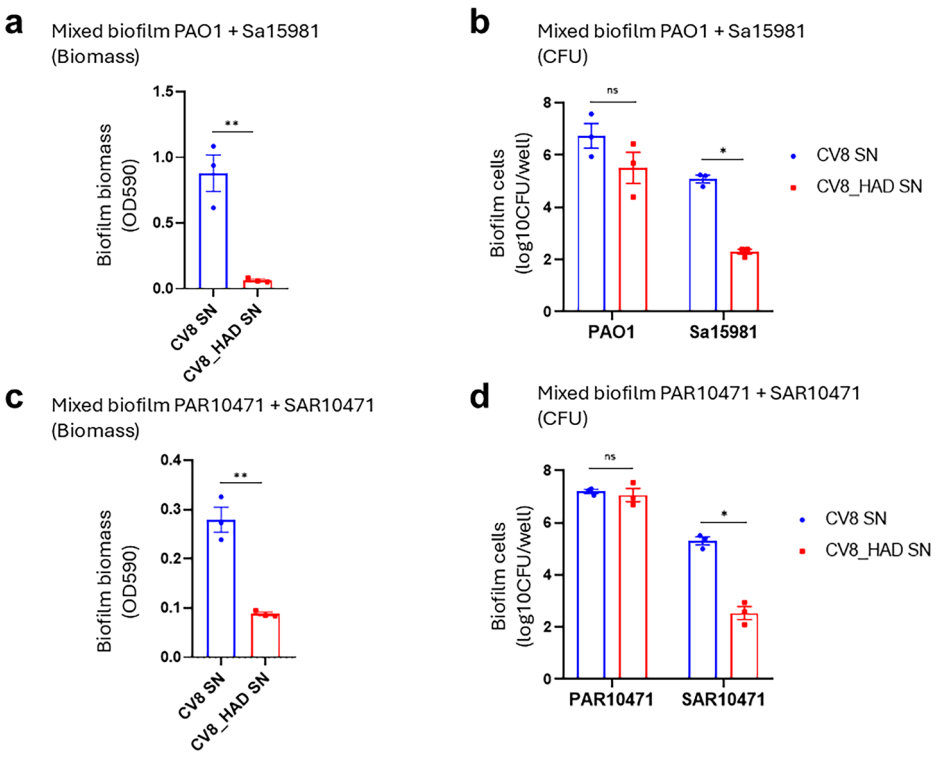

Fig. 2 | CV8_HAD dissolves dual-species biofilms in vitro. a, **c** Biofilms were obtained by co-culturing *P. aeruginosa* and *S. aureus* in 96-wells for 24 h at 37 °C in static conditions. Then, biofilms were washed and treated with supernatants (SN) from CV8_HAD or the control strain CV8 for six hours and subsequently quantified by crystal violet as detailed in the Materials and methods. **b**, **d** The proportion of *P. aeruginosa* and *S. aureus* viable bacteria in the mixed biofilms was assessed after each treatment by direct seeding on MacConkey Agar or Mannitol Salt Agar, respectively. Data shown are the mean ± SEM ($n = 3$) and statistical significance by Student's *t*-test: $^{**}p < 0.01$; $^{***}p < 0.001$.

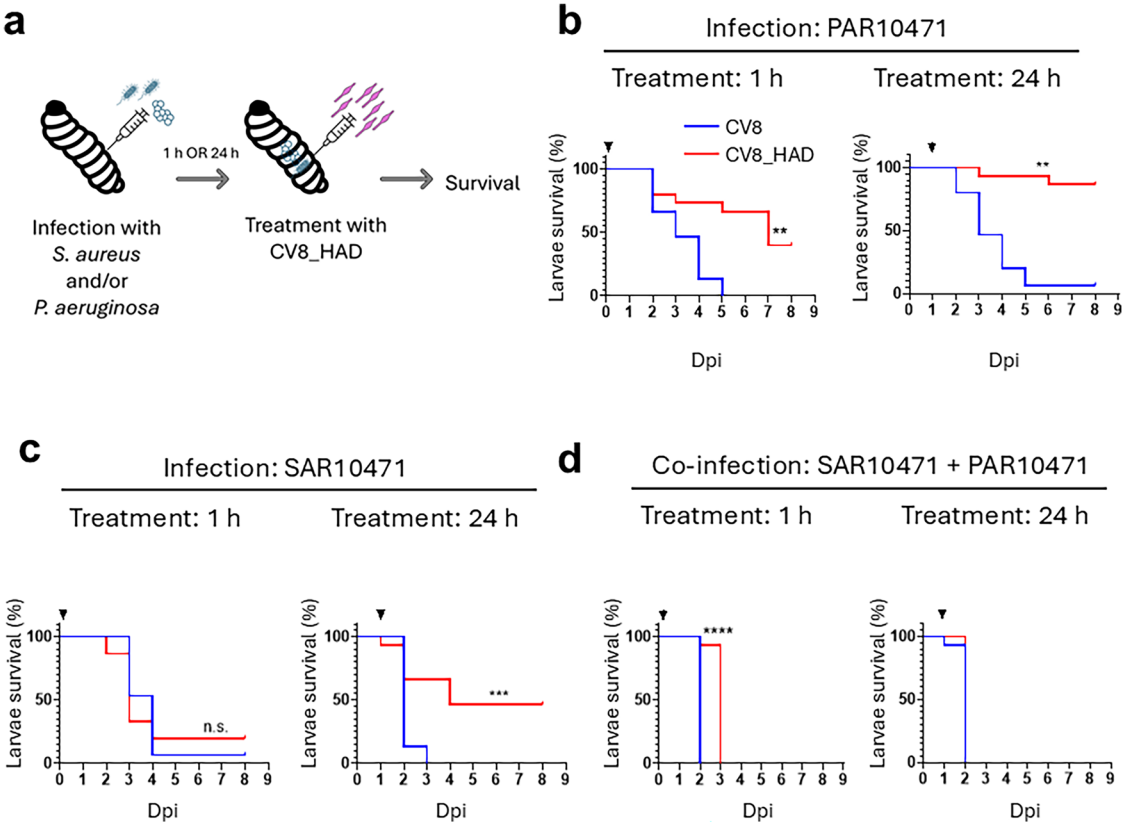

Fig. 3 | CV8_HAD increases the survival of *G. mellonella* larvae infected with *S. aureus* and/or *P. aeruginosa*. **a** Schematic representation of the experiments carried out in larvae. Briefly, *G. mellonella* larvae ($n = 15$) were infected with different isolates of *S. aureus* and/or *P. aeruginosa*, and treated 1 or 24 hpi with 10^7 CFU of CV8_HAD; one group (n = 15) treated with CV8 was used as negative control. Survival was monitored daily for eight days post-treatment (dpi), and graphically represented by a Kaplan-Meyer survival curve. Results obtained in larvae infected with bacterial strains: (**b**) PAR10471 (5×10^2 CFU), **c** SAR10471 (10^6 CFU), or **d** a combination of SAR10471 and PAR10471 (10^6 CFU and 5×10 CFU, respectively). Statistical comparisons were performed by the Log-rank (Mantel-Cox) test: n.s. = not significant; * $p = 0.024$; ** $p = 0.005$; **** $p < 0.0001$.

but showed efficacy when administered at 24 hpi (four days vs. two days; Fig. 3c).

Larvae co-infected with SAR10471 and PAR10471 exhibited markedly higher mortality compared to single infections (approximately 100% mortality at 48 h; Fig. 3d), most likely due to synergistic effects, as previously reported[13]. In line with this, CV8_HAD treatment was not effective in co-infected larvae when administered at 24 hpi; however, it significantly delayed larval mortality when administered at 1 hpi (Fig. 3d), indicating that early administration of CV8_HAD is required to counteract biofilm-associated virulence in co-infected larvae. The efficacy of CV8_HAD was further confirmed in larvae infected with strain Sa15981 (Supplementary Fig. 6), a strain that forms robust biofilm in vitro.

Taken together, our results demonstrate the efficacy of CV8_HAD as a therapeutic agent against *P. aeruginosa and S. aureus mono- and dual-species* biofilm, not only in vitro but also in vivo in the *G. mellonella* larvae model.

Discussion

Bacterial biofilms play an important role in a range of diseases in pulmonary and critical care medicine, such as catheter-associated infections, ventilator-associated pneumonia, and chronic infections in cystic fibrosis[45]. In fact, an estimated 60% of chronic or recurrent respiratory infections are directly associated with bacterial biofilms, increasing patient morbidity and mortality rates and economic burdens[5]. Biofilms create structures hindering bacteria from the activity of antibiotics, immune system and other external stressors, requiring treatments at high doses of antibiotics for long-lasting periods that, despite it, frequently result in relapses with poor prognosis. The presence of polymicrobial biofilms represents an additional complication, being *P. aeruginosa* and *S. aureus* the agents more frequently found in chronic and acute respiratory complex diseases[6–13]. One interesting approach to solve these clinical problems consists of the development of new treatments directed to combine the biofilm dispersal with low doses of antibiotics, allowing more rational and effective treatments[32,33]. Moreover, biofilm dispersants can disrupt the planktonic propagation lifestyle of the bacteria egressed from a mature biofilm, making these bacteria more susceptible to drugs and the host immune system.

Supporting this promising strategy, we present here a new therapeutic approach based on an attenuated live bacterium, called CV8_HAD, expressing simultaneously enzymes that target alginate, polysaccharides Pel and Psl, and PNAG polymers. We first demonstrated CV8_HAD anti-biofilm activity against single- and dual-species biofilm in vitro; then, we validated CV8_HAD antibiofilm activity in a well-established *S. aureus* biofilm murine model using a subcutaneously implanted sealed catheter.

Given the difficulty and lack of reliability of in vivo mice models with *P. aeruginosa* biofilms, we finally validated the CV8_HAD in vivo activity using *G. mellonella* larvae, which represents a low-cost, reliable, and ethically preferred model for testing novel antimicrobials[44]. This insect model is increasingly used to evaluate antimicrobial compounds, but its potential for studying antibiofilm agents and engineered therapeutic bacteria remains largely unexplored. While previous studies have shown that *S. aureus* can form biofilms on pre-implanted abiotic surfaces inside *G. mellonella* larvae[46], biofilm formation in larvae without the use of devices has not yet been described. In our study, we provide evidence of device-free biofilm formation in larvae. First, we demonstrated that the payloads secreted by CV8_HAD do not inhibit planktonic bacterial growth (Supplementary Fig. 3). Therefore, its therapeutic efficacy in larvae is likely attributable to

interference with biofilm-associated virulence. Second, we observed variability in treatment efficacy across bacterial strains depending on the timing of administration (1 or 24 hpi; Fig. 3). This variability correlates with the strains' ability to form biofilm in vitro (Supplementary Fig. 2): strains with a higher biofilm-forming capacity (PAR10471 and Sa15981) responded better to early treatment administration (1 hpi) compared to low biofilm-forming strains (such as SAR10471). Third, confocal microscopy revealed tightly packed aggregates of bacilli-shaped bacteria within *P. aeruginosa*-infected larvae at 24 hpi, consistent with the presence of a biofilm (Supplementary Fig. 7). Collectively, these findings strongly suggest that both *S. aureus* and *P. aeruginosa* form biofilm-like aggregates within *G. mellonella* larvae, consistent with biofilm development observed in other animal models, three-dimensional lung epithelial cell system[47], or even in biological fluids[48–54].

Importantly, our results establish a novel application of the *G. mellonella* infection model for screening the efficacy of antibiofilm compounds delivered via live biotherapeutic products (LBP). Indeed, the optimal dosage and timing of LPB administration must be carefully optimized, considering several factors, including LBP persistence within the larvae, the intrinsic ability of the infecting strain to form aggregates or biofilm, the bacterial load in single infections, and the relative ratio of each species in co-infections. In our experimental setting, the limited CV8_HAD persistence in larvae, which decreases by three orders of magnitude beyond 24 hpi, combined with the strain-dependent timing of biofilm formation, likely explains the variability in treatment efficacy observed when administration occurred at either 1 or 24 hpi.

A key limitation of using larval survival as a readout to screen for antibiofilm activity is that biofilm-associated virulence represents only a subset of the overall pathogenicity of a bacterium. Both *S. aureus*[55] and *P. aeruginosa*[56] produce a wide array of virulence factors beyond those involved in biofilm formation. Consequently, even when biofilm formation is successfully impaired, other virulence mechanisms may still cause larval death, potentially leading to an underestimation of the antibiofilm efficacy of the treatment being evaluated. This likely explains why, despite the therapeutic efficacy of CV8_HAD, larval mortality was still observed in our experiments.

Noteworthy, the alginate, polysaccharides Pel and Psl, and PNAG polymers biofilm matrix components disaggregated by CV8_HAD are not exclusive of *S. aureus* and *P. aeruginosa* biofilms. Evidences suggest that Pel is a common biofilm matrix component in many Gram-positive bacteria, as the core *pelDEA*$_{DA}$*FG* locus is conserved across diverse species of bacilli, clostridia, streptococci, and actinobacteria[57]. In fact, PelAh from *P. aeruginosa* has been shown to disrupt Pel-based biofilm formed by the *Bacillus cereus*[57]. Similarly, the PNAG biosynthesis pathway has been characterized in multiple bacteria species[58–62] and the enzyme dispersin B has been reported to disperse biofilms formed by *Staphylococcus epidermidis*, *Escherichia coli* K-12[63], *Bordetella bronchiseptica*, and *Bordetella pertussis*[64], among others[65]. These findings support the hypothesis that CV8_HAD may degrade biofilms formed by a wide range of pathogenic bacteria in the context of complex multispecies biofilm in vivo.

Bacterial antibiotic resistance has reached a critical stage, coinciding with a marked decline in the pharmaceutical industry's development of novel antibiotics. As conventional antibiotics become less reliable, alternative treatment strategies need to be explored to ensure effective therapies against bacterial infections. Over the last decade, monoclonal antibodies targeting bacterial toxins, including *S. aureus*' α-hemolysin, have been undergoing clinical trials[66–68]. Bacteriophages therapies are also under consideration not only in in vivo models[69] but also in clinical trials[70–72], demonstrating effectiveness of phage treatment against *P. aeruginosa* and *S. aureus* infections.

Another innovative approach for treating bacterial infections is represented by engineered live bacteria. Preclinical studies described the engineering of *E. coli* Nissle 1917 to fight pathogenic bacteria in the gut, *e.g.*, by expressing a microcin against *Salmonella* spp[73]., antimicrobial peptides against *Enterococcus* spp[74]., or pyocin S5 against *P. aeruginosa*[75]. Acid lactic bacteria have also been engineered against intestinal infections, *e.g. Lactococcus lactis* secreting antimicrobial peptides against pathogenic *E. coli* and *Salmonella* infections[76], or *Lactobacillus casei* expressing *Listeria* adhesion proteins to reduce *L. monocytogenes* mucosal colonization[77]. While all these new approaches are designed to target infections in the intestinal tract, no engineered live bacteria have been reported to tackle respiratory infections. In this regard, *M. pneumoniae* offers many advantages as a chassis for treatment of respiratory infections: (i) its natural niche are the airways; (ii) as it lacks of a cell wall, it can be combined with antibiotics targeting the peptidoglycan layer of pathogens[33]; (iii) its negligible genome recombination rate reduces the risk of gene horizontal transfer; (iv) its UGA codon encodes for tryptophan instead of a translation stop, providing an intrinsic biocontainment mechanism; and (v) it can be grown in a defined, synthetic, serum-free medium to upscale its good manufacturing practice-compliant production[78].

In conclusion, given the intrinsic properties of *M. pneumoniae* as a delivery vector, the previously demonstrated attenuation of the CV8 chassis in murine lungs[40], and the ability of CV8_HAD to secrete antibiofilm compounds effective against multispecies biofilms, we highlight the translational promise of CV8_HAD as a novel living therapeutic for combating biofilm-associated antimicrobial resistance. While the present study does not use a respiratory infection model, our findings provide a foundation for future work in this direction. Specifically, upcoming studies will evaluate the efficacy of CV8_HAD in relevant respiratory models. In a clinical context, we envision CV8_HAD as a candidate therapeutic product for patients with chronic or recurrent respiratory infections characterized by *P. aeruginosa* and *S. aureus* biofilm formation, such as CF, COPD, and VAP. Formulated as an inhalable suspension for respiratory delivery (e.g., via nebulizer, dry powder inhaler, or intranasal spray), CV8_HAD could promote biofilm dispersal in the airways, allowing its combination with lower doses of antibiotics and enabling more rational and effective antimicrobial therapies.

Methods

Bacterial strains, media, and growth conditions

A list of the bacterial strains used in this work and their original description reference is in Table 1. Strains *P. aeruginosa* PAR10471 and *S. aureus* SAR10471 are clinical isolates from a patient suffering respiratory problems[13]. The attenuated strain CV8 derives from the wild-type *M. pneumoniae* strain M129 (ATCC 29342, subtype 1), in which genes mpn133 and mpn372 were deleted, and the *mpn051* gene was replaced by the *gpsA* gene from *Mycoplasma penetrans*[40].

M. pneumoniae strains were cultured in T75 flasks (VWR) with 25 ml of modified Hayflick medium (here called Hayflick) and incubated at 37 °C in a 5% CO_2 supplement until the late exponential phase. Hayflick was prepared with: 18.4 g/L of PPLO broth (Difco), 100 mM HEPES, 0.0025% phenol red (Sigma-Aldrich), and NaOH to pH 7.75 supplemented after autoclaving with 20% heat-inactivated horse serum (Life Technologies), 55 mM glucose, and 100 ug/mL ampicillin (Sigma-Alrich). When required, bacto agar 1% (BD) was added before sterilization to prepare the solid version, as well as the antibiotics for selection (all from Sigma-Aldrich): tetracycline (2 µg/ml) or chloramphenicol (20 µg/ml). Unless otherwise specified, *P. aeruginosa* and *S. aureus* strains were precultured in LB agar plates and cultured routinely in tryptic soy broth (TSB; BD Difco) and subsequent incubation at 37 °C, 600 rpm, overnight.

For *P. aeruginosa* and *S. aureus* in vitro growth curve assays, bacteria were grown overnight in TSB medium at 37 °C on shaking. The next day, the cultures were diluted to a OD600 of 0.1, and this suspension was added to 96-wells in the presence of 10% or 40% of CV8 or CV8_HAD supernatant. The plate was incubated in a TECAN plate reader (Infinite 200 Pro) at 37 °C on shaking, and the OD600 was read every 20 min. To obtain the supernatants, *M. pneumoniae* was cultured in a T25 flask filled with 5 ml of Hayflick medium (free from antibiotics). After flask incubation at 37 °C for three days, the SN was harvested in a 1.5 mL tube, centrifuged at 17000 g at

4 °C for 10 min, and filtered by 0.22-µm (Millipore). This method allows the obtention of a cell-free SN, as assessed by direct plating on Hayflick-agar medium. The cell-free SN was kept at 4 °C or −20 °C until its use.

For *M. pneumoniae* in vitro growth curve, cell suspensions were inoculated into 96-well plates and incubated statically at 37 °C in a TECAN plate reader (Infinite 200 Pro). Absorbance at 430 nm and 560 nm was measured every 2 h. The growth index at each time point was calculated as the ratio of 430/560 nm, reflecting the colour change of the culture medium due to acidification, which correlates with an increase in biomass, as previously described[79,80]. Doubling times of the strains were calculated as ln(2)/slope of the curve, considering the timepoints in the exponential phase only.

For *M. pneumoniae* maintenance in mice lungs, C57BL/6 mice were intratracheally inoculated with 5 × 107 CFU of CV8 ($n = 17$) or CV8_HAD ($n = 10$); the lungs were harvested at 2 and 4 days after inoculation, homogenized, serial diluted, and seeded onto Hayflick-agar plates. After 10 days at 37 °C, colonies on the plates were counted.

Plasmids and generation of CV8 recombinant mutants

The CV8 recombinant mutants were generated by transforming mini-transposon vectors by electroporation.

The mini-transposons vectors were generated by fusing the synthetic promoter prEF-Tu to the selected enzymes genes (PelAh, PslGh, A1-II', and/or DspB) containing the signal peptide mpn142opt[32] at their N-termini for secretion. Assembling of these vectors was made following the Gibson method[79]. When required, gene fragments were synthesized by IDT Corporation. Oligonucleotides were synthesized by Sigma-Aldrich, and the PCR reactions were performed with Phusion DNA polymerase (Thermo Fisher Scientific). The final sequence of all the plasmids was confirmed by Sanger sequencing (Eurofins Genomics).

To transform the mini-transposons, CV8 was cultured in T75 culture flasks with 25 mL Hayflick medium at 37 °C and 5% CO2 until late exponential phase. Cells were washed twice in precooled electroporation buffer (272 mM sucrose, Hepes 8 mM, pH 7.4), scraped in 1 ml electroporation buffer, collected in a 1.5 ml tube, and homogenized by rinsing ten times through a 25-gauge syringe needle. Then, 50 µl of cell suspension were mixed with 1.5 µg of the corresponding plasmid in a 0.1-cm cuvette, which was kept on ice for 20 min, submitted to electroporation (Biora Gene Pulser Xcell Electroporation Systems) at 1250 V/25 µF/100 Ω, and immediately diluted in 420 µl of fresh Hayflick. The suspension obtained was transferred to a 1.5 ml tube, incubated at 37 °C for 3 h, and finally inoculated into a T25 plate with 5 ml Hayflick supplemented with the antibiotic for selection (tetracycline (2 µg/ml) or chloramphenicol (20 µg/ml). Resistant cells usually expand within seven days of the transformation.

Western blot

To obtain cell lysates, cells growing in T75 flasks in exponential phase were lysed with 1 ml SDS 4% (Sigma) and Hepes 100 mM (Sigma), and sonicated (Bioruptor Plus from Diagenode) for 10 min on HIGH position with an interval ON/OFF of 30 sec on ice. Samples were subjected to SDS–PAGE on a Novex™ 4–12% Bis-Tris Protein Gels in MOPS running buffer (ThermoFisher), transferred to nitrocellulose membranes with an iBlot 3 Western Blot Transfer Systems (ThermoFisher), blocked with 5% skim milk (Sigma), hybridized with polyclonal primary antibodies (customized by Proteogenix) and then with HRP-conjugated secondary antibodies (anti-rabbit IgG, Sigma A0545). After incubating the membrane with the HRP substrate (ThermoFisher Pico), the chemiluminescent signal was detected with an iBright CL750 Imaging System (ThermoFisher).

In vitro biofilm degradation assay

M. pneumoniae was cultured in a T25 flask filled with 5 ml of Hayflick medium (free from antibiotics). After flask incubation at 37 °C for three days, the SN was harvested in a 1.5 mL tube, centrifuged at 17000 g at 4 °C for 10 min, and filtered by 0.22-µm (Millipore). This method allows the obtention of a cell-free SN, as assessed by direct plating on Hayflick-agar medium. The cell-free SN was kept at 4 °C or −20 °C until its use.

On the other hand, *P. aeruginosa* and *S. aureus* cultures were grown in TSB (37 °C, 600 rpm, overnight) by mixing 20 µl of stock in 20 ml of TSB, then diluted to an $OD_{600} = 0.15$ in the same broth culture, and distributed (100 µl/well, in triplicate) into sterile 96-well polystyrene microtiter plates (VWR). The plates were incubated at 37 °C, statically, for 24 h to allow biofilm formation, and then washed with PBS to remove nonadherent cells cells and the biofilms formed were treated with 100 µl/well of *M. pneumoniae* SN for 6 h, at 37 °C. After incubation, the wells were washed with PBS and stained with 150 µl of 0.1% Crystal Violet (Sigma) solution in water, followed by three washes with PBS. The stained biofilm was solubilized by adding 100 µl of 95% ethanol and incubating for 10 min. Absorbance was read at OD 595 nm using a TECAN plate reader (Infinite 200 Pro).

Also, the effect of CV8_HAD SN on *P. aeruginosa* and *S. aureus* viability was assessed by CFU/ml enumeration by resuspending the adhered cells in 200 µl/well of PBS, serial dilution, and plating (100 µl/dilution, triplicate) on Mannitol Salt Agar (Condalab) or MacConkey Agar (Condalab) or LB agar. The plates were incubated (37 °C, 24 h) and the mean ± SD (n = 3) of CFU/ml was calculated and statistically compared by ANOVA and the pos-hoc Least Significant Differences (LSD) tests, using GraphPad Prism 8.0.1.

In vivo efficacy of CV8_HAD on catheter-associated biofilms by [^{18}F]FDG-Micro-PET in mice

Female CD1 outbreed mice (Charles River International) of 20–22 grams body weight were accommodated with water and food *ad libitum* in the animal facilities of the Institute of Agrobiotechnology (REGA ES/31-2010-000013). Mouse handling and procedures were performed by accredited personnel, in compliance with the current European and national regulations, following the FELASA and ARRIVE welfare guidelines, with the authorization of the competent authority of the Navarra Government (codes 281/2020 and 282/2020).

S. aureus biofilm infection was monitored by the [^{18}F]FDG-MicroPET imaging in the previously developed and validated mouse model[42]. Upon arrival, CD1 mice were acclimated for one week and randomly allocated to cages. Sealed vialon® catheters were precolonized with Sa15981 and subcutaneously implanted in CD1 mice ($n = 5$); 24 h later, all mice were treated with a single subcutaneous injection of CV8_HAD or CV8 as an untreated control; and 1 and 4 days after treatment, biofilm signal was monitored by intravenous injection of 18.8–1.9 MBq of [^{18}F]FDG). To achieve this, PET images were acquired 1 hour after radiotracer administration, over a 15-minute period, using a MicroPET scanner (Mosaic; Philips, USA). Mice were maintained under anaesthesia with 2% isoflurane in oxygen during imaging. The images were reconstructed using a true 3D RAMLA algorithm. The MicroPET images were analyzed using the PMOD software (PMOD Technologies Ltd., Adliswil, Switzerland), and semiquantitative results were expressed as the Standardized Uptake Value (SUV) index, obtained as detailed[42]. After qualitative inspection of the images, volumes of interest (VOI) were manually drawn on coronal 1-mm-thick consecutive layers including the entire catheter area. For catheter image quantification, manual bias of surrounding areas was avoided by a semi-automatically generated new VOI, using the threshold of 60% maximum pixel for SUV mean calculation (SUV60 index). Imaging Unit personnel were blinded to group allocation while performing MicroPET scans. As established in our previous works, SUV60 signal is a quantitative estimation of the bacterial abundance, immune cell infiltration, and inflammation. Accordingly, the efficacy of CV8_HAD treatment was determined by the mean SUV60 values ($n = 5$) detected in CV8_HAD vs. CV8 control groups, as well as the mean SUV60 values variations from 1 to 4 days after treatment, in each mice group. Statistical comparisons of SUV60 values were performed by Student's t-test (GraphPad Prism 8.0.1).

Survival of *Galleria mellonella* larvae

The larvae of *Galleria mellonella* were obtained from our own hatchery, and included in the infection assay according to the following criteria:: healthy-looking aspect, weighing around 200–300 mg, and no signs of melanization.

To prepare the inocula, *P. aeruginosa* and *S. aureus* isolates were grown overnight at 37 °C in 10 mL of LB or 0.5X TSB supplemented with 1% glucose, respectively, as optimized in previous studies[13,80]. Then, cells were centrifuged at 5000 g, washed in PBS, and adjusted to the desired cell dose required to kill *G. mellonella* over a 24–96 h period, as determined in previous studies. The selected doses ranged from 10^1 to 10^2 cfu per larvae for *P. aeruginosa*, and from 10^6 to 4×10^7 CFU per larvae for *S. aureus* isolates. For the co-infections, the same bacterial burden of *P. aeruginosa* and *S. aureus* as the individual infections was used. Fifteen larvae per group were infected through the left proleg with 10 µL of each bacterial suspension using a 50 µl Hamilton Microliter syringe and incubated in the dark at 37 °C in empty petri dishes. One or twenty-four hours later, larvae were treated with 10^7 CFU/larvae of CV8-HAD or the control strain CV8. The exact number of bacteria inoculated was confirmed retrospectively by ten-fold serial dilutions in PBS; plating (100 ml/dilution, triplicate) on LB agar medium; and incubation of plates for 24 h, at 37 °C. Larvae mortality was monitored daily for eight days, considering that a larva was dead when showing these three features: no response to touching, absence of cocoon, and black melanization colour, following a standard scoring method[81]. The cumulative survival curves were determined by Kaplan-Meier and statistically compared by the log-rank (Mantel-Cox) test, using GraphPad Prism 8.0.1.

G. mellonella larvae processing and imaging

Larvae were fixed in formaldehyde (24 h at 4 °C), washed (3 times, 15 min each, at 4 °C), cryopreserved in 30% sucrose (5 days at 4 °C), and transferred to O.C.T. compound for 46 h at 4 °C. Samples were then frozen on dry ice, embedded in O.C.T. in cryo-moulds, and stored at −80 °C until cryosectioning. Longitudinal sections (10 µm thick) were obtained from the medial region of the larvae using a cryostat (Leica CM3050S). Sections were mounted on pre-treated slides, dried for 40 min on a heated plate at 37 °C (Leica HI1220), washed in PBS (3 × 5 min), and counterstained with Hoechst 33342 (trihydrochloride trihydrate). Images were acquired using confocal microscopy (Zeiss LSM980) at 63× magnification.

Data availability

All the raw data are available on request (Western Blot original images, absorbances values of the crystal violet assays, CFU countings on plates, SUV60 values of the Micro-PET, counting of larvae survival, original images of the confocal microscopy).

Received: 1 April 2025; Accepted: 25 September 2025;
Published online: 17 November 2025

References

1. Naghavi, M. et al. Global burden of bacterial antimicrobial resistance 1990–2021: a systematic analysis with forecasts to 2050. *Lancet* **404**, 1199–1226 (2024).
2. *WHO Bacterial Priority Pathogens List 2024: Bacterial Pathogens of Public Health Importance, to Guide Research, Development, and Strategies to Prevent and Control Antimicrobial Resistance*. (World Health Organization, Geneva, 2024).
3. Zhao, A., Sun, J. & Liu, Y. Understanding bacterial biofilms: From definition to treatment strategies. *Front. Cell. Infect. Microbiol.* **13**, 1137947 (2023).
4. Sharma, S. et al. Microbial biofilm: a review on formation, infection, antibiotic resistance, control measures, and innovative treatment. *Microorganisms* **11**, 1614 (2023).
5. Assefa, M. & Amare, A. Biofilm-associated multi-drug resistance in hospital-acquired infections: a review. *Infect. Drug Resist.* **15**, 5061–5068 (2022).
6. Tilouche, L. et al. Staphylococcus aureus ventilator-associated pneumonia: a study of bacterio-epidemiological profile and virulence factors. *Curr. Microbiol.* **78**, 2556–2562 (2021).
7. Torres, A. et al. International ERS/ESICM/ESCMID/ALAT guidelines for the management of hospital-acquired pneumonia and ventilator-associated pneumonia: Guidelines for the management of hospital-acquired pneumonia (HAP)/ventilator-associated pneumonia (VAP) of the European Respiratory Society (ERS), European Society of Intensive Care Medicine (ESICM), European Society of Clinical Microbiology and Infectious Diseases (ESCMID) and Asociación Latinoamericana del Tórax (ALAT). *Eur. Respir. J.* **50**, 1700582 (2017).
8. Rello, J., Lisboa, T. & Koulenti, D. Respiratory infections in patients undergoing mechanical ventilation. *Lancet Respir. Med.* **2**, 764–774 (2014).
9. Hatziagorou, E. et al. Changing epidemiology of the respiratory bacteriology of patients with cystic fibrosis–data from the European cystic fibrosis society patient registry. *J. Cyst. Fibros.* **19**, 376–383 (2020).
10. Coburn, B. et al. Lung microbiota across age and disease stage in cystic fibrosis. *Sci. Rep.* **5**, 10241 (2015).
11. Engler, K. et al. Colonisation with Pseudomonas aeruginosa and antibiotic resistance patterns in COPD patients. *Swiss Med. Wkly*. https://doi.org/10.4414/smw.2012.13509 (2012).
12. Marsh, R. L. et al. Detection of biofilm in bronchoalveolar lavage from children with non-cystic fibrosis bronchiectasis. *Pediatr. Pulmonol.* **50**, 284–292 (2015).
13. Gomes-Fernandes, M. et al. Strain-specific interspecies interactions between co-isolated pairs of Staphylococcus aureus and Pseudomonas aeruginosa from patients with tracheobronchitis or bronchial colonization. *Sci. Rep.* **12**, 3374 (2022).
14. Biswas, L., Biswas, R., Schlag, M., Bertram, R. & Götz, F. Small-colony variant selection as a survival strategy for *Staphylococcus aureus* in the presence of *Pseudomonas aeruginosa*. *Appl. Environ. Microbiol.* **75**, 6910–6912 (2009).
15. Mashburn, L. M., Jett, A. M., Akins, D. R. & Whiteley, M. *Staphylococcus aureus* Serves as an Iron Source for *Pseudomonas aeruginosa* during In Vivo Coculture. *J. Bacteriol.* **187**, 554–566 (2005).
16. Abisado, R. G., Benomar, S., Klaus, J. R., Dandekar, A. A. & Chandler, J. R. Bacterial Quorum sensing and microbial community interactions. *mBio* **9**, e02331–17 (2018).
17. Millette, G. et al. Despite Antagonism in vitro, Pseudomonas aeruginosa Enhances Staphylococcus aureus colonization in a murine lung infection model. *Front. Microbiol.* **10**, 2880 (2019).
18. Orazi, G. & O'Toole, G. A. *Pseudomonas aeruginosa* Alters *Staphylococcus aureus* sensitivity to Vancomycin in a biofilm model of cystic fibrosis infection. *mBio* **8**, e00873–17 (2017).
19. Frydenlund Michelsen, C. et al. Evolution of metabolic divergence in *Pseudomonas aeruginosa* during long-term infection facilitates a proto-cooperative interspecies interaction. *ISME J.* **10**, 1323–1336 (2016).
20. Hoffman, L. R. et al. Selection for *Staphylococcus aureus* small-colony variants due to growth in the presence of *Pseudomonas aeruginosa*. *Proc. Natl Acad. Sci.* **103**, 19890–19895 (2006).
21. Hotterbeekx, A., Kumar-Singh, S., Goossens, H. & Malhotra-Kumar, S. In vivo and In vitro Interactions between Pseudomonas aeruginosa and Staphylococcus spp. *Front. Cell. Infect. Microbiol*. **7**, 1–13 (2017).
22. Alves, P. M. et al. Interaction between Staphylococcus aureus and Pseudomonas aeruginosa is beneficial for colonisation and pathogenicity in a mixed biofilm. *Pathog. Dis*. **76**, 1–10 (2018).
23. Limoli, D. H. & Hoffman, L. R. Help, hinder, hide and harm: what can we learn from the interactions between *Pseudomonas aeruginosa* and *Staphylococcus aureus* during respiratory infections?. *Thorax* **74**, 684–692 (2019).
24. Hubert, D. et al. Association between Staphylococcus aureus alone or combined with Pseudomonas aeruginosa and the clinical condition of patients with cystic fibrosis. *J. Cyst. Fibros.* **12**, 497–503 (2013).
25. Limoli, D. H. et al. Staphylococcus aureus and Pseudomonas aeruginosa co-infection is associated with cystic fibrosis-related diabetes and poor clinical outcomes. *Eur. J. Clin. Microbiol. Infect. Dis.* **35**, 947–953 (2016).

26. Maliniak, M. L., Stecenko, A. A. & McCarty, N. A. A longitudinal analysis of chronic MRSA and Pseudomonas aeruginosa co-infection in cystic fibrosis: A single-center study. *J. Cyst. Fibros.* **15**, 350–356 (2016).
27. Blackledge, M. S., Worthington, R. J. & Melander, C. Biologically inspired strategies for combating bacterial biofilms. *Curr. Opin. Pharmacol.* **13**, 699–706 (2013).
28. Donelli, G. et al. Synergistic activity of Dispersin B and Cefamandole Nafate in inhibition of Staphylococcal biofilm growth on polyurethanes. *Antimicrob. Agents Chemother.* **51**, 2733–2740 (2007).
29. Tuon, F. F. et al. Antimicrobial Treatment of Staphylococcus aureus Biofilms. *Antibiotics* **12**, 87 (2023).
30. Xu, Y. et al. Antibiofilm effects of punicalagin against Staphylococcus aureus in vitro. *Front. Microbiol.* **14**, 1175912 (2023).
31. Valliammai, A., Selvaraj, A., Yuvashree, U., Aravindraja, C. & Karutha Pandian, S. sarA-dependent antibiofilm activity of thymol enhances the antibacterial efficacy of Rifampicin against Staphylococcus aureus. *Front. Microbiol.* **11**, 1744 (2020).
32. Garrido, V. et al. Engineering a genome-reduced bacterium to eliminate Staphylococcus aureus biofilms in vivo. *Mol. Syst. Biol.* **17**, e10145 (2021).
33. Mazzolini, R. et al. Engineered live bacteria suppress Pseudomonas aeruginosa infection in mouse lung and dissolve endotracheal-tube biofilms. *Nat. Biotechnol.* **41**, 1089–1098 (2023).
34. Yin, R., Cheng, J., Wang, J., Li, P. & Lin, J. Treatment of Pseudomonas aeruginosa infectious biofilms: Challenges and strategies. *Front. Microbiol.* **13**, 955286 (2022).
35. Lefebvre, E., Vighetto, C., Di Martino, P., Larreta Garde, V. & Seyer, D. Synergistic antibiofilm efficacy of various commercial antiseptics, enzymes and EDTA: a study of Pseudomonas aeruginosa and Staphylococcus aureus biofilms. *Int. J. Antimicrob. Agents* **48**, 181–188 (2016).
36. Daboor, S. M., Raudonis, R. & Cheng, Z. Characterizations of the viability and gene expression of dispersal cells from Pseudomonas aeruginosa biofilms released by alginate lyase and tobramycin. *PLOS ONE* **16**, e0258950 (2021).
37. Fanaei Pirlar, R. et al. Combinatorial effects of antibiotics and enzymes against dual-species Staphylococcus aureus and Pseudomonas aeruginosa biofilms in the wound-like medium. *PLOS ONE* **15**, e0235093 (2020).
38. Wang, Z. et al. Repurposing DNase I and alginate lyase to degrade the biofilm matrix of dual-species biofilms of Staphylococcus aureus and Pseudomonas aeruginosa grown in artificial sputum medium: In-vitro assessment of their activity in combination with broad-spectrum antibiotics. *J. Cyst. Fibros*. S1569199324000274, https://doi.org/10.1016/j.jcf.2024.02.012 (2024).
39. Srivastava, R. & Lesser, C. F. Living engineered bacterial therapeutics: emerging affordable precision interventions. *Microb. Biotechnol.* **17**, e70057 (2024).
40. Montero-Blay, A. et al. Bacterial expression of a designed single-chain IL-10 prevents severe lung inflammation. *Mol. Syst. Biol.* **19**, e11037 (2023).
41. Blanco-Cabra, N. et al. Characterization of different alginate lyases for dissolving Pseudomonas aeruginosa biofilms. *Sci. Rep.* **10**, 9390 (2020).
42. Garrido, V. et al. In vivo monitoring of staphylococcus aureus biofilm infections and antimicrobial therapy by [18F] Fluoro-Deoxyglucose-MicroPET in a Mouse Model. *Antimicrob. Agents Chemother.* **58**, 6660–6667 (2014).
43. Valle, J. et al. SarA and not σ^B is essential for biofilm development by *Staphylococcus aureus*. *Mol. Microbiol.* **48**, 1075–1087 (2003).
44. Ménard, G., Rouillon, A., Cattoir, V. & Donnio, P.-Y. Galleria mellonella as a suitable model of bacterial infection: past, present and future. *Front. Cell. Infect. Microbiol.* **11**, 782733 (2021).
45. Boisvert, A.-A., Cheng, M. P., Sheppard, D. C. & Nguyen, D. Microbial biofilms in pulmonary and critical care diseases. *Ann. Am. Thorac. Soc.* **13**, 1615–1623 (2016).
46. Campos-Silva, R., Brust, F. R., Trentin, D. S. & Macedo, A. J. Alternative method in Galleria mellonella larvae to study biofilm infection and treatment. *Microb. Pathog.* **137**, 103756 (2019).
47. Crabbé, A. et al. Antimicrobial efficacy against Pseudomonas aeruginosa biofilm formation in a three-dimensional lung epithelial model and the influence of fetal bovine serum. *Sci. Rep.* **7**, 43321 (2017).
48. Douglas, S. I., Williams, J. O. & Onyedibia, G. C. Isolation of biofilm producing bacteria from stool samples and their antibiogram. *Microbiol. Infect. Dis*. **6**, 1–9 (2022).
49. De Waele, J. J. et al. The role of abdominal drain cultures in managing abdominal infections. *Antibiotics* **11**, 697 (2022).
50. Souza, L. C. D. et al. Association between pathogens from tracheal aspirate and oral biofilm of patients on mechanical ventilation. *Braz. Oral Res*. **31**, 1–9 (2017).
51. Perez-Tanoira, R. et al. Bacterial biofilm in salivary stones. *Eur. Arch. Otorhinolaryngol.* **276**, 1815–1822 (2019).
52. Mounier, R. et al. Biofilm-associated infection: the hidden face of cerebrospinal fluid shunt malfunction. *Acta Neurochir,* **158**, 2321–2324 (2016).
53. Pinto, H., Simões, M. & Borges, A. Prevalence and impact of biofilms on bloodstream and urinary tract infections: a systematic review and meta-analysis. *Antibiotics* **10**, 825 (2021).
54. Drago, L. et al. Dithiotreitol pre-treatment of synovial fluid samples improves microbiological counts in peri-prosthetic joint infection. *Int. Orthop.* **47**, 1147–1152 (2023).
55. Girma, A. Staphylococcus aureus: Current perspectives on molecular pathogenesis and virulence. *Cell Surf.* **13**, 100137 (2025).
56. Qin, S. et al. Pseudomonas aeruginosa: pathogenesis, virulence factors, antibiotic resistance, interaction with host, technology advances and emerging therapeutics. *Signal Transduct. Target. Ther*. **7**, 1–27 (2022).
57. Whitfield, G. B. et al. Discovery and characterization of a Gram-positive Pel polysaccharide biosynthetic gene cluster. *PLOS Pathog.* **16**, e1008281 (2020).
58. Cerca, N. et al. Protection against *Escherichia coli* infection by antibody to the *Staphylococcus aureus* poly- *N* -acetylglucosamine surface polysaccharide. *Proc. Natl Acad. Sci.* **104**, 7528–7533 (2007).
59. Chen, K.-M. et al. The role of pgaC in Klebsiella pneumoniae virulence and biofilm formation. *Microb. Pathog.* **77**, 89–99 (2014).
60. Bentancor, L. V., O'Malley, J. M., Bozkurt-Guzel, C. & Pier, G. B. Maira-Litrán, T. Poly- *N* -Acetyl-β-(1-6)-Glucosamine is a target for protective immunity against Acinetobacter baumannii infections. *Infect. Immun.* **80**, 651–656 (2012).
61. Yakandawala, N. et al. Characterization of the Poly-β-1,6- *N* -Acetylglucosamine Polysaccharide component of Burkholderia biofilms. *Appl. Environ. Microbiol.* **77**, 8303–8309 (2011).
62. Wang, X., Preston, J. F. & Romeo, T. The *pgaABCD* Locus of *Escherichia coli* promotes the synthesis of a polysaccharide adhesin required for biofilm formation. *J. Bacteriol.* **186**, 2724–2734 (2004).
63. Itoh, Y., Wang, X., Hinnebusch, B. J., Preston, J. F. & Romeo, T. Depolymerization of β-1,6- *N* -Acetyl- D -Glucosamine disrupts the integrity of diverse bacterial biofilms. *J. Bacteriol.* **187**, 382–387 (2005).
64. Parise, G., Mishra, M., Itoh, Y., Romeo, T. & Deora, R. Role of a putative polysaccharide Locus in *Bordetella* biofilm development. *J. Bacteriol.* **189**, 750–760 (2007).
65. Izano, E. A., Amarante, M. A., Kher, W. B. & Kaplan, J. B. Differential Roles of Poly- *N* -Acetylglucosamine Surface Polysaccharide and Extracellular DNA in *Staphylococcus aureus* and *Staphylococcus epidermidis* Biofilms. *Appl. Environ. Microbiol.* **74**, 470–476 (2008).

66. Henrique, I. D. M. et al. Therapeutic antibodies against shiga toxins: trends and perspectives. *Front. Cell. Infect. Microbiol.* **12**, 825856 (2022).
67. Mohamed, M. F. H. et al. Efficacy, safety, and cost-effectiveness of Bezlotoxumab in preventing recurrent clostridioides difficile infection: systematic review and meta-analysis. *J. Clin. Gastroenterol.* **58**, 389–401 (2024).
68. Ruzin, A. et al. Performance of the Cepheid Methicillin-Resistant Staphylococcus aureus/S. aureus skin and soft tissue infection PCR assay on respiratory samples from mechanically ventilated patients for S. aureus screening during the Phase 2 Double-Blind SAATELLITE Study. *J. Clin. Microbiol.* **60**, e00347–22 (2022).
69. Tagliaferri, T. L., Jansen, M. & Horz, H.-P. Fighting pathogenic bacteria on two fronts: phages and antibiotics as combined strategy. *Front. Cell. Infect. Microbiol.* **9**, 22 (2019).
70. Merabishvili, M. et al. Stability of bacteriophages in burn wound care products. *PLOS ONE* **12**, e0182121 (2017).
71. Furfaro, L. L., Payne, M. S. & Chang, B. J. Bacteriophage therapy: clinical trials and regulatory hurdles. *Front. Cell. Infect. Microbiol.* **8**, 376 (2018).
72. Jault, P. et al. Efficacy and tolerability of a cocktail of bacteriophages to treat burn wounds infected by Pseudomonas aeruginosa (PhagoBurn): a randomised, controlled, double-blind phase 1/2 trial. *Lancet Infect. Dis.* **19**, 35–45 (2019).
73. Palmer, J. D. et al. Engineered probiotic for the inhibition of Salmonella via Tetrathionate-induced production of Microcin H47. *ACS Infect. Dis.* **4**, 39–45 (2019).
74. Geldart, K. G. et al. Engineered *E. coli* Nissle 1917 for the reduction of vancomycin-resistant *Enterococcus* in the intestinal tract. *Bioeng. Transl. Med.* **3**, 197–208 (2018).
75. Hwang, I. Y. et al. Engineered probiotic Escherichia coli can eliminate and prevent Pseudomonas aeruginosa gut infection in animal models. *Nat. Commun.* **8**, 15028 (2017).
76. Volzing, K., Borrero, J., Sadowsky, M. J. & Kaznessis, Y. N. Antimicrobial peptides targeting gram-negative pathogens, produced and delivered by lactic acid bacteria. *ACS Synth. Biol.* **2**, 643–650 (2013).
77. Drolia, R. et al. Receptor-targeted engineered probiotics mitigate lethal Listeria infection. *Nat. Commun.* **11**, 6344 (2020).
78. Gaspari, E. et al. Model-driven design allows growth of Mycoplasma pneumoniae on serum-free media. *Npj Syst. Biol. Appl.* **6**, 33 (2020).
79. Gibson, D. G. et al. Enzymatic assembly of DNA molecules up to several hundred kilobases. *Nat. Methods* **6**, 343–345 (2009).
80. Kwasny, S. M. & Opperman, T. J. Static biofilm cultures of gram-positive pathogens grown in a microtiter format used for anti-biofilm drug discovery. *Curr. Protoc. Pharmacol*. **50**, 1–26 (2010).
81. Tsai, C. J.-Y., Loh, J. M. S. & Proft, T. *Galleria mellonella* infection models for the study of bacterial diseases and for antimicrobial drug testing. *Virulence* **7**, 214–229 (2016).

Acknowledgements

This work was supported by SNEO 20211019 (2021; Neotec; CDTI), and EUR2023-143461 (Spanish Ministry of Science and Innovation and Universities) grants. RM acknowledges to Spanish Ministry of Science and Innovation for the PTQ2020-011049 grant. ML-S also acknowledges to Talent UAB-Banc Santander programme and the Scientific Foundation of the Spanish Association Against Cancer (project reference LAB_LA-BAE247377LLUC) to support her role as principal investigator in the Synthetic biology group at UAB. A-CG, IG and DY also acknowledge to Spanish Ministry of Science and Innovation (PID2023-150290OB-I00) and the Catalan AGAUR (2021 SGR00092).

Author contributions

R.M. designed and performed experiments, analysed data and wrote the paper. V.G., A.-C.G., D.Y. designed and performed experiments. M.C., C.P.-L., I.G., and M.J.G. gave technical support and conceptual advice. M.L.-S. designed experiments, analysed data, gave technical support and conceptual advice, wrote the paper,and led the project. All authors read and approved the final manuscript.

Competing interests

The results published in this article are covered by patents EP3262061A1/US10745450B2, EP4121445/US20230310564/JP2023518294 and EP4405488/US20240382537 (licensed to Pulmobiotics S.L). ML-S is one of the shareholders of Pulmobiotics. RM, CP-L and ML-S are employees and have stock options of Pulmobiotics S.L. The remaining authors declare no competing interests.

Additional information

Supplementary information The online version contains supplementary material available at https://doi.org/10.1038/s41522-025-00835-2.

Correspondence and requests for materials should be addressed to Rocco Mazzolini or Maria Lluch-Senar.